Crystal Structures of Di-iron μ-η^2-(C,C)-Ketene Complexes, $[\{Fe(\eta^5\text{-}C_5H_5)(CO)_2\}_2(\mu\text{-}CH_2CO)]$ and $[\{Fe(\eta^5\text{-}C_5Me_5)(CO)_2\}_2(\mu\text{-}CH_2CO)]$. Synergistic Metal-to-Ligand Back Donation as revealed by Comparison with $[\{Fe(\eta^5\text{-}C_5H_5)(CO)_2\}_2(\mu\text{-}CH_2CH_2CO)]$†

Munetaka Akita,* Atsuo Kondoh, and Yoshihiko Moro-oka*
Research Laboratory of Resources Utilization, Tokyo Institute of Technology, 4259 Nagatsuta, Midori-ku, Yokohama 227, Japan

The solid-state structures of di-iron μ-ketene complexes $[\{Fe(\eta^5\text{-}C_5H_5)(CO)_2\}_2(\mu\text{-}CH_2CO)]$ (**1**) and $[\{Fe(\eta^5\text{-}C_5Me_5)(CO)_2\}_2(\mu\text{-}CH_2CO)]$ (**2**) and of a reference complex, $[\{Fe(\eta^5\text{-}C_5H_5)(CO)_2\}_2(\mu\text{-}CH_2CH_2CO)]$ (**3**), have been determined by single-crystal *X*-ray diffraction. In accord with previous spectroscopic studies, the geometry of the bridging ketene ligands reflects three resonance structures. In particular, the contribution of the π-complex form is verified based on the observations that the CH_2–CO bond is shortened and the $CH_2C{=}O$ bond is elongated compared with the situation in complex (**3**) which lacks the π-complex form. The geometry around the metal centres is determined by the need to minimize steric repulsions among ancillary ligands, and does not reflect orbital interactions.

The structure and chemical behaviour of ketene ligands in polymetallic systems[1] have been attracting much attention, because ketene species are often referred to as an origin of oxygenated products in catalytic hydrogenation of carbon monoxide.[2] We

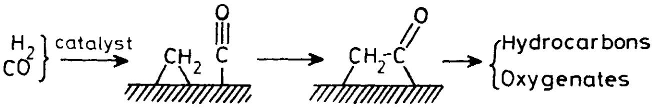

previously reported the preparation, spectroscopic characterization, and reactivities of heterobimetallic μ-η^2-(C,C)-ketene complexes, $(OC)_2(\eta^5\text{-}C_5H_5)Fe{-}CH_2CO{-}ML_n$ (M = Fe, Co, Ni, Mn, Mo; L = $\eta^5\text{-}C_5H_5$, CO, PR_3)[3] Spectroscopic studies show that the structures of these binuclear μ-ketene complexes may be regarded as 1,4-dimetalla-2-butanones (**A**) without mutual interaction between Fe and M. Furthermore, i.r. studies

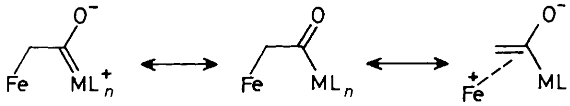

(**B**) (**A**) (**C**)

reveal a significant contribution of the π-complex resonance form (**C**) in addition to the oxycarbene structure (**B**) which is well established for mononuclear acyl complexes. The structure (**C**) arises from d_π–p_π back donation from the metal centre β to the acyl carbonyl group (so-called β effect).[4]

In this article we describe the results of structural determinations of the complexes $[\{Fe(\eta^5\text{-}C_5H_5)(CO)_2\}_2(\mu\text{-}CH_2CO)]$ (**1**) and $[\{Fe(\eta^5\text{-}C_5Me_5)(CO)_2\}_2(\mu\text{-}CH_2CO)]$ (**2**), and a μ-oxopropanediyl complex, $[\{Fe(\eta^5\text{-}C_5H_5)(CO)_2\}_2(\mu\text{-}CH_2CH_2CO)]$ (**3**), by single-crystal *X*-ray diffraction. Since (**3**) lacks a π-resonance form like (**C**) which is suitable for back donation, substantial differences are observed between (**1**), (**2**), and (**3**). Complexes (**1**) and (**2**) are the third examples of structurally characterized μ-η^2-(C,C)-ketene complexes.[5,6]

Experimental

All manipulations were performed under an argon atmosphere by using standard Schlenk-tube techniques. The analytical facilities used and the preparation of complexes (**1**) and (**3**) have been described previously.[3] After thrice repeated recrystallization from diethyl ether–hexane, (**1**) contained one molecule of water.

Preparation of Complex (**2**).[3]—Treatment of $[Fe(\eta^5\text{-}C_5Me_5)(CO)_2(CH_2CO_2H)]$[7] (2.75 g, 9.0 mmol) in CH_2Cl_2 (5 cm^3) with oxalyl dichloride (1.1 cm^3, 15 mmol) resulted in vigorous gas evolution. After 10 min the volatiles were removed under reduced pressure. To the residue dissolved in tetrahydrofuran (thf) (10 cm^3) and cooled at −78 °C was added a thf solution (50 cm^3) generated by reduction of $[\{Fe(\eta^5\text{-}C_5Me_5)(CO)_2\}_2]$ (2.65 g, 5.4 mmol) by $NaK_{2.8}$ alloy (1 g). After stirring for 1 h at room temperature the solvent was removed under reduced pressure. Extraction with ether and column chromatography on alumina (activity II–III: Merck Art. 1097) afforded the above dimer [purple band eluted with CH_2Cl_2–hexane (1 : 5)] followed by a yellow band (eluted with CH_2Cl_2) from which complex (**2**) (1.45 g, 2.71 mmol, 50% yield) was isolated as yellow crystals after recrystallization from ether–hexane, m.p. 173 °C (Found: C, 58.20; H, 6.00. $C_{26}H_{32}Fe_2O_5$ requires C, 58.25; H, 6.00%); $\nu(C{\equiv}O)$ 1 992, 1 977, 1 932, and 1 933 cm^{-1}, $\nu(C{=}O)$ 1 585 cm^{-1} (CH_2Cl_2); $\delta_H(C_6D_6)$ 1.43, 1.67 (15 H × 2, s, C_5Me_5), and 2.35 (2 H, s, CH_2); δ_C 9.09 [q, *J*(CH) 127.5, C_5Me_5], 9.72 [q, *J*(CH) 127.2, C_5Me_5], 41.17 [t, *J*(CH) 133.6, CH_2], 94.81, 96.95 (s × 2, C_5Me_5), 218.65, 218.87 (s × 2, Fe–C≡O), and 260.90 p.p.m. [t, ^2J(CH) 3.0 Hz, CH_2CO].

Structure Analyses and Refinement.—Diffraction measurements were made on a Rigaku AFC-5 automated four-circle diffractometer by using graphite-monochromated Mo-K_α radiation (λ = 0.710 68 Å). Unit cells were determined and refined by a least-squares method using 20 independent reflections with

---

† μ-Ketene-C^1(Fe^1)C^2(Fe^2)-bis[dicarbonyl(η-cyclopentadienyl)iron], -bis[dicarbonyl(η-pentamethylcyclopentadienyl)iron], and μ-1-oxopropane-1,3-diyl-bis[dicarbonyl(η-cyclopentadienyl)iron].

Supplementary data available: see Instructions for Authors, *J. Chem. Soc., Dalton Trans.*, 1989, Issue 1, pp. xvii—xx.

Table 1. Crystallographic data[a]

Compound	(1)·H_2O	(2)	(3)
Formula	$C_{16}H_{14}Fe_2O_6$	$C_{26}H_{32}Fe_2O_5$	$C_{17}H_{14}Fe_2O_5$
a/Å	9.811 0(20)	10.210 2(16)	7.986 7(109)
b/Å	14.071 7(23)	16.546 9(19)	19.630 7(30)
c/Å	7.043 1(10)	8.337(34)	6.783 1(85)
α/°	98.407(17)	92.602(24)	91.103(47)
β/°	97.525(19)	101.616(28)	127.803(55)
γ/°	119.956(11)	108.243(11)	91.006(48)
U/Å^3	809.46(28)	1 301.40(62)	839.56(168)
M	414.0	536.2	410.0
D_c/g cm^{-3}	1.70	1.37	1.62
μ(Mo-K_α)	17.316	10.825	16.651
F(000)	414	536	410
Crystal size/mm	0.20 × 0.30 × 0.35	0.20 × 0.25 × 0.30	0.15 × 0.25 × 0.35
No. of reflections with $F > 3\sigma(F)$	3 990	4 395	3 422
R	5.22	8.56	6.63
R'[b]	5.18	9.50	7.39

[a] Details common to all three complexes: triclinic; space group $P\bar{1}$; $Z = 2$. [b] $R' = [\Sigma w(|F_o| - |F_c|)^2/\Sigma w|F_o|^2]^{\frac{1}{2}}$.

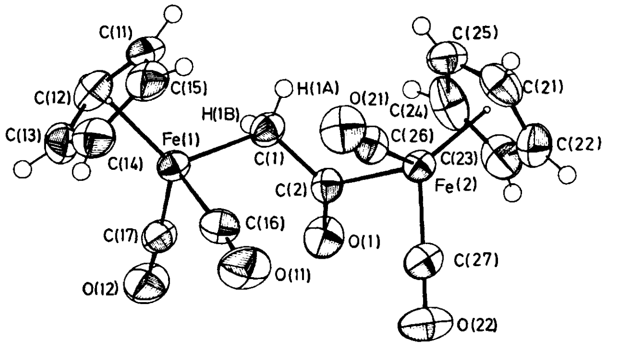

Figure 1. Molecular structure of complex (**1**) with thermal ellipsoids at the 50% probability level

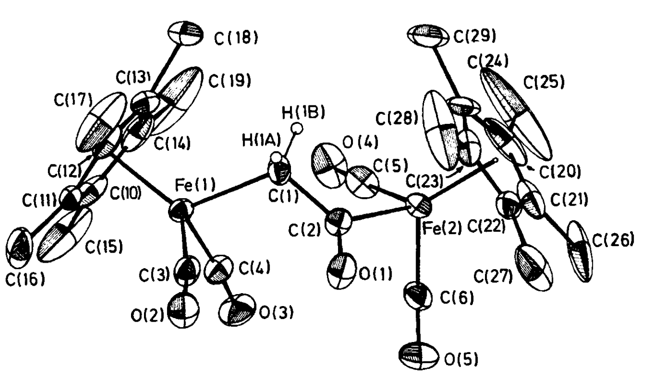

Figure 2. Molecular structure of complex (**2**) with thermal ellipsoids at the 20% probability level

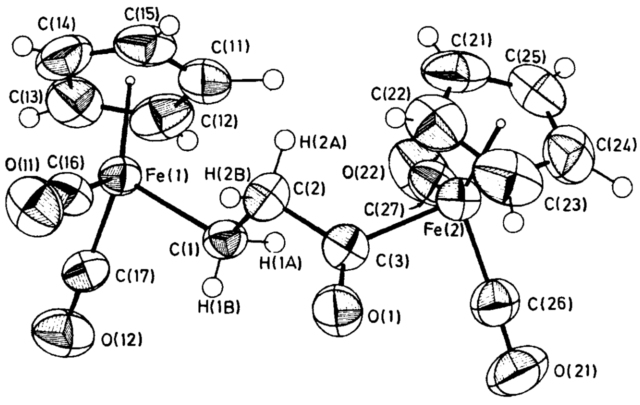

Figure 3. Molecular structure of complex (**3**) with thermal ellipsoids at the 50% probability level

$25 < 2\theta < 30°$. Data were collected over the range $2 < 2\theta < 60°$ with the ω—2θ scan technique and the scan speed was 6° min^{-1}. If $\sigma(F)/F$ was more than 0.1, a scan was repeated up to three times and the results were added to the first scan. Three standard reflections were monitored every 100 measurements. Crystal data, data-collection parameters, and results of the analyses are listed in Table 1. All data processing was performed on a FACOM A-70 computer by using the R-CRYSTAN structure-solving program obtained from Rigaku Corp. Neutral scattering factors were obtained from the standard sources.[8] In reducing the data, Lorentz and polarization corrections were made but no absorption correction. Full-matrix least-squares refinements minimized the function $[\Sigma w(|F_o| - |F_c|)^2/\Sigma w|F_o|^2]^{\frac{1}{2}}$ where $w = 1/[\sigma(F_o)^2 + (pF_o)^2]$, the parameter p being automatically optimized.

All the compounds (**1**)—(**3**) crystallized in the triclinic system ($P\bar{1}$). The positions of the Fe atoms were located by the Patterson method for (**1**) and (**3**) and by the direct method for (**2**). Subsequent Fourier difference maps revealed the positions of all other atoms of (**1**) and (**3**) and all non-hydrogen atoms of (**2**). For (**1**) and (**3**) all atoms were refined with anisotropic thermal parameters for non-hydrogen atoms and with isotropic thermal parameters for hydrogen atoms. For (**2**) all non-hydrogen atoms were refined anisotropically and only two methylene protons on the ketene bridge were refined isotropically.

Additional material available from the Cambridge Crystallographic Data Centre comprises H-atom co-ordinates, thermal parameters, and remaining bond lengths and angles.

Results and Discussion

ORTEP drawings of complexes (**1**)—(**3**) are reproduced in Figures 1—3, positional parameters in Tables 2—4 and selected bond lengths and bond angles in Tables 5 and 6. The molecular structures of (**1**) and (**2**) confirm that the ketene complexes obtained by our preparative method adopt the 1,4-dimetalla-2-butanone structure without mutual interaction between two iron atoms [Fe••• Fe 4.450(1) Å for (**1**) and 4.521(2) Å for (**2**)]

Table 2. Positional parameters for non-hydrogen atoms of complex (**1**)·H_2O

Atom	X/a	Y/b	Z/c
CP1[a]	0.784 36	0.229 25	0.738 14
CP2[b]	1.481 85	0.267 73	1.220 60
Fe(1)	0.857 52(6)	0.218 28(5)	0.965 76(7)
Fe(2)	1.344 93(6)	0.305 38(5)	1.277 60(7)
C(1)	1.024 26(56)	0.168 55(38)	0.985 54(63)
C(2)	1.107 40(47)	0.186 86(32)	1.190 75(57)
C(11)	0.869 67(68)	0.205 96(53)	0.664 09(68)
C(12)	0.711 99(68)	0.129 10(44)	0.678 44(71)
C(13)	0.652 43(60)	0.189 67(47)	0.772 28(75)
C(14)	0.772 76(69)	0.305 16(47)	0.820 95(77)
C(15)	0.910 33(68)	0.316 36(47)	0.754 93(77)
C(16)	0.961 17(54)	0.329 61(38)	1.181 94(68)
C(17)	0.740 16(52)	0.120 48(37)	1.094 70(59)
C(21)	1.568 47(62)	0.358 90(44)	1.197 34(87)
C(22)	1.576 84(60)	0.328 26(47)	1.371 58(81)
C(23)	1.453 38(69)	0.213 54(50)	1.339 22(92)
C(24)	1.370 82(63)	0.173 86(44)	1.143 50(102)
C(25)	1.439 76(71)	0.264 09(53)	1.051 34(71)
C(26)	1.322 62(50)	0.408 40(35)	1.189 41(63)
C(27)	1.312 79(53)	0.339 21(35)	1.509 84(66)
O(1)	1.039 66(35)	0.125 09(25)	1.295 97(46)
O(11)	1.016 73(47)	0.401 77(31)	1.321 62(53)
O(12)	0.658 38(41)	0.060 18(29)	1.178 05(50)
O(21)	1.316 55(41)	0.478 90(26)	1.132 28(50)
O(22)	1.288 60(44)	0.359 12(29)	1.663 32(50)
O(2)	1.214 36(50)	0.076 14(37)	1.605 31(65)

[a] CP1: centroid of C(11)–C(15). [b] CP2: centroid of C(21)–C(25).

Table 3. Positional parameters for non-hydrogen atoms of complex (**2**)

Atom	X/a	Y/b	Z/c
CP1[a]	0.101 55	0.915 54	0.127 23
CP2[b]	0.388 25	0.588 05	0.425 50
Fe(1)	0.161 70(10)	0.877 82(6)	0.309 37(11)
Fe(2)	0.265 41(10)	0.639 75(6)	0.444 36(13)
C(1)	0.300 80(81)	0.809 41(54)	0.317 36(121)
C(2)	0.324 01(77)	0.767 84(47)	0.468 30(93)
C(3)	0.270 24(89)	0.941 73(53)	0.489 52(99)
C(4)	0.054 47(84)	0.804 39(54)	0.416 08(99)
C(5)	0.104 33(89)	0.624 72(53)	0.304 32(120)
C(6)	0.193 45(93)	0.639 59(54)	0.617 54(120)
C(10)	−0.011 78(95)	0.901 34(95)	0.159 80(133)
C(11)	0.099 51(133)	0.977 97(65)	0.207 76(93)
C(12)	0.214 48(86)	0.966 85(59)	0.143 86(108)
C(13)	0.170 44(121)	0.887 01(66)	0.057 29(99)
C(14)	0.035 10(130)	0.844 55(62)	0.067 44(114)
C(15)	−0.155 96(126)	0.880 59(157)	0.187 98(213)
C(16)	0.105 03(227)	1.059 58(90)	0.299 28(139)
C(17)	0.363 81(118)	1.035 60(102)	0.156 25(187)
C(18)	0.246 42(227)	0.849 03(129)	−0.049 07(158)
C(19)	−0.049 70(228)	0.751 62(84)	−0.020 11(178)
C(20)	0.297 86(106)	0.527 98(84)	0.353 69(246)
C(21)	0.346 57(123)	0.539 97(62)	0.512 44(191)
C(22)	0.450 02(99)	0.615 96(62)	0.556 21(102)
C(23)	0.473 23(87)	0.655 16(53)	0.419 38(147)
C(24)	0.373 59(148)	0.601 16(111)	0.285 80(108)
C(25)	0.179 92(157)	0.451 18(129)	0.250 76(397)
C(26)	0.295 77(200)	0.477 15(101)	0.630 31(294)
C(27)	0.526 29(194)	0.643 31(126)	0.736 27(158)
C(28)	0.589 25(136)	0.735 14(86)	0.413 50(323)
C(29)	0.353 56(313)	0.608 61(206)	0.106 32(166)
O(1)	0.382 79(68)	0.808 15(35)	0.601 91(72)
O(2)	0.338 24(74)	0.991 25(41)	0.601 91(77)
O(3)	−0.022 17(68)	0.761 09(46)	0.484 23(84)
O(4)	−0.002 50(65)	0.608 87(44)	0.210 68(99)
O(5)	0.152 08(90)	0.640 48(53)	0.734 85(95)

[a] CP1: centroid of C(10)–C(14). [b] CP2: centroid of C(20)–C(24).

Table 4. Positional parameters for non-hydrogen atoms of complex (**3**)

Atom	X/a	Y/b	Z/c
CP1[a]	−0.325 37	0.369 61	0.062 56
CP2[b]	0.160 04	0.110 73	−0.137 80
Fe(1)	−0.056 93(10)	0.378 07(2)	0.308 74(11)
Fe(2)	0.191 43(10)	0.128 59(3)	0.135 40(13)
C(11)	−0.305 44(78)	0.312 35(35)	0.020 13(118)
C(12)	−0.347 37(90)	0.333 66(41)	0.181 24(133)
C(13)	−0.362 09(87)	0.404 73(38)	0.177 32(133)
C(14)	−0.323 67(101)	0.427 47(37)	0.014 60(139)
C(15)	−0.288 28(90)	0.369 83(41)	−0.080 50(115)
C(16)	0.135 15(80)	0.430 68(28)	0.334 33(93)
C(17)	0.051 05(77)	0.390 83(26)	0.620 87(98)
C(21)	0.012 79(121)	0.146 23(50)	−0.246 50(115)
C(22)	0.223 49(145)	0.168 06(41)	−0.127 08(142)
C(23)	0.349 34(121)	0.109 22(50)	−0.016 47(142)
C(24)	0.208 08(132)	0.053 73(40)	−0.080 58(138)
C(25)	0.006 52(118)	0.076 42(41)	−0.218 37(124)
C(26)	0.359 27(93)	0.089 00(31)	0.421 57(109)
C(27)	−0.012 50(81)	0.133 88(29)	0.160 81(96)
C(1)	0.141 66(77)	0.297 44(25)	0.410 09(93)
C(2)	0.186 09(95)	0.279 50(29)	0.227 64(111)
C(3)	0.328 34(77)	0.217 95(26)	0.313 75(96)
O(1)	0.516 40(56)	0.225 13(19)	0.476 33(78)
O(11)	0.259 22(72)	0.466 09(23)	0.352 87(87)
O(12)	0.118 82(71)	0.399 49(25)	0.826 36(77)
O(21)	0.470 92(84)	0.064 15(26)	0.611 88(87)
O(22)	0.151 13(63)	0.135 47(25)	0.170 53(87)

[a] CP1: centroid of C(11)–C(15). [b] CP2: centroid of C(21)–C(25).

Table 5. Selected intramolecular bond lengths (Å) for complexes (**1**)—(**3**)

	(**1**)	(**2**)	(**3**)
C–C(Cp1)$_{av.}$[a]	1.409	1.400	1.393
C–C(Cp2)$_{av.}$[b]	1.396	1.366	1.400
C(Cp1)–Me$_{av.}$[a]		1.527	
C(Cp2)–Me$_{av.}$[b]		1.505	
C(Cp1)–Fe(1)$_{av.}$[a]	2.106	2.108	2.099
C(Cp2)–Fe(2)$_{av.}$[b]	2.109	2.102	2.107
CP1–Fe(1)[c]	1.729	1.739	1.732
CP2–Fe(2)[d]	1.742	1.752	1.738
Fe(1)–C(16)[C(3)][e]	1.764(4)	1.748(7)	1.750(7)
Fe(1)–C(17)[C(4)][e]	1.761(4)	1.768(9)	1.739(6)
Fe(2)–C(26)[C(5)][e]	1.755(6)	1.753(9)	1.753(6)
Fe(2)–C(27)[C(6)][e]	1.749(5)	1.747(11)	1.744(8)
C(16)–O(11)[C(3)–O(2)][e]	1.145(5)	1.159(9)	1.140(9)
C(17)–O(12)[C(4)–O(3)][e]	1.139(6)	1.146(11)	1.152(8)
C(26)–O(21)[C(5)–O(4)][e]	1.149(7)	1.152(10)	1.152(7)
C(27)–O(22)[C(6)–O(5)][e]	1.161(6)	1.142(14)	1.150(10)
Fe(1)–C(1)	2.073(7)	2.068(10)	2.071(5)
C(1)–C(2)	1.481(6)	1.474(13)	1.519(12)
C(2)–C(3)			1.534(8)
C(2)–O(1)[C(3)–O(1)][f]	1.219(5)	1.208(9)	1.203(5)
C(2)–Fe(2)[C(3)–Fe(2)][f]	2.008(3)	2.002(8)	1.992(5)

[a] Cp1: C(11)–C(15) for (**1**) and (**3**), C(10)–C(14) for (**2**). [b] Cp2: C(21)–C(25) for (**1**) and (**3**), C(20)–C(24) for (**2**). [c] CP1: centroid of C(11)–C(15) for (**1**) and (**3**) and C(10)–C(14) for (**2**). [d] CP2: centroid of C(21)–C(25) for (**1**) and (**3**) and C(20)–C(24) for (**2**). [e] For complex (**2**). [f] For complex (**3**).

as anticipated from spectroscopic studies. The structure of (**3**) is described as a 1,5-dimetalla-2-pentanone [Fe • • • Fe 5.682(1) Å].

The geometry of Fe(η^5-C_5H_5)(CO)$_2$ in complexes (**1**) and (**3**) is a typical three-legged piano-stool structure with the OC–Fe–CO and R–Fe–CO (R = CH_2 or C=O) angles being approximately right angles. The bond lengths and angles [C–C(C_5H_5) 1.364—1.434, Fe–C(C_5H_5) 2.081—2.130, Fe–CO 1.739—1.764, and C–O 1.139—1.161 Å; C–C–C(C_5H_5) 106.48—

109.48, OC–Fe–CO 92.54—94.84, OC–Fe–R (CH_2 or C=O) 87.61—95.74, and C_5H_5–Fe–CO or R 117.87—128.22°] fall in the ranges of those reported for Fe(η^5-C_5H_5)$(CO)_2$ (M′)-alkyl complexes [M′–CH_2CO_2H,[4] M′–$CH_2COC_5H_4$Fe(η^5-C_5H_5),[9] M′–σ-C_5H_5,[10] M′–$(CH_2)_n$–M′ (n = 3 or 4),[11] M′–$(CH{=}CH)_2$–M′[12]] and an acyl complex [M′–COCH=PMe_3;[13] C–C(C_5H_5) 1.30—1.45, Fe–C(C_5H_5) 1.98—2.26, Fe–CO 1.66—1.78, and C–O 1.13—1.17 Å; C–C–C(C_5H_5) 102—115, OC–Fe–CO 89—96, OC–Fe–R 86—92, and C_5H_5–Fe–CO 122—127°]. No significant and systematic differences in the structure between the Fe(η^5-C_5H_5)$(CO)_2$ groups on the alkyl and acyl sides in complexes (**1**) and (**3**) is observed. Similarly, the structure of the Fe(η^5-C_5Me_5)$(CO)_2$ parts in (**2**) [C–C(C_5Me_5) 1.299—1.440, C(C_5Me_5)–Me 1.473—1.572, Fe–C(C_5Me_5) 2.080—2.132, Fe–CO 1.747—1.768, and C–O 1.142—1.159 Å; C–C–C(C_5Me_5) 105.71—110.11, OC–Fe–CO 93.82(37), 94.00(46), OC–Fe–R 89.22—94.66, and C_5Me_5–Fe–CO or R 120.39—126.19°] is essentially the same (also the three-legged piano-stool structure) as that of a rare example of an Fe(η^5-C_5Me_5)$(CO)_2$ (M″)-alkyl complex M″–C_5H_5.[14]

Interatomic distances and bond angles of the bridging ketene and oxopropanediyl ligands are summarized in Table 7. The Fe–C(acyl) bond lengths are shorter than the Fe–C(alkyl) lengths by 0.07 Å. This value is greater than the difference in bond lengths between sp^3 and sp^2 carbon atoms (0.04 Å).[15] Therefore shortening of the Fe–C(acyl) bond arises from the oxycarbene resonance form (**B**). Bond angles associated with the bridging ligands demonstrate that the methylene and acyl carbons are sp^3 and sp^2 hybridized, respectively.

It should be also noted that the CH_2–CO bond distances of μ-ketene complexes (**1**) [1.481(6) Å] and (**2**) [1.474(13) Å] are substantially shorter (*ca.* 0.05 Å) than that of (**3**) [1.534(8) Å] and acyl iron complexes [Fe$(CO)_2${HB$(pz)_3$}–COMe (pz = pyrazolyl),[16] 1.522(8); Fe(η^5-C_5H_5)(CO)(PPh_3)–COMe,[17] 1.531(15) Å] and, on the contrary, that the C=O bond distances of (**1**) [1.219(5) Å] and (**2**) [1.208(9) Å] are slightly longer than that of (**3**) [1.203(5) Å]. The latter compares with hitherto reported acyl C=O bond distances: Fe$(CO)_2${HB$(pz)_3$}–COMe, 1.193(6); Fe(η^5-C_5H_5)(CO)(PPh_3)–COMe, 1.228(13); Fe(η^5-C_5H_5)(CO)(PPh_3)–COPh,[18] 1.22(3); and Fe(η^5-C_5H_5)$(CO)_2$–COCH = PMe_3,[13] 1.234 Å. Electron-donating groups such as PPh_3 on metal centres and PMe_3 on an α-carbon of the acyl group elongate the C=O bonds. In Figure 4 the Newman projection of complex (**1**) along the C(1)–C(2) is shown. The dihedral angles θ between the acyl C=O plane and the C(2)–Fe(2) plane are 75.6 and 67.8°, respectively. As a whole, the conformations observed for (**1**) and (**2**) should maximize the

Table 6. Selected intramolecular bond angles (°) for complexes (**1**)—(**3**)

	(**1**)	(**2**)	(**3**)
C–C–C$(Cp1)_{av.}$[a]	108.00	107.99	108.00
C–C–C$(Cp2)_{av.}$[b]	108.00	107.98	107.99
C–C(Cp1)–$Me_{av.}$[a]		125.95	
C–C(Cp2)–$Me_{av.}$[b]		125.95	
Fe(1)–C(16)–O(11)	174.31(57)	172.70(86)	
[Fe(1)–C(3)–O(2)][c]			178.53(61)
Fe(1)–C(17)–O(12)	175.66(58)		178.70(66)
[Fe(1)–C(4)–O(3)][c]		174.19(94)	
Fe(2)–C(26)–O(21)	176.43(39)		178.73(49)
[Fe(2)–C(5)–O(4)][c]		175.21(89)	
Fe(2)–C(27)–O(22)	178.44(40)		177.40(52)
[Fe(2)–C(6)–O(5)][c]		177.10(77)	
CP1–Fe(1)–C(16)[C(3)][c,d]	125.15(20)	125.38(30)	128.22(16)
CP1–Fe(1)–C(17)[C(4)][c,d]	124.97(14)	125.63(26)	125.16(22)
CP1–Fe(1)–C(1)[d]	118.19(13)	120.26(29)	121.29(12)
CP2–Fe(2)–C(26)[C(5)][c,e]	123.97(17)	126.19(34)	127.36(28)
CP2–Fe(2)–C(27)[C(6)][c,e]	128.20(19)	123.17(34)	125.84(16)
CP2–Fe(2)–C(2)[C(3)][c,e]	118.30(15)	120.39(25)	117.87(23)
Fe(1)–C(1)–C(2)	113.99(38)	115.08(69)	114.61(36)
C(1)–C(2)–C(3)			110.87(53)
C(1)–C(2)–Fe(2)	117.08(29)	117.63(52)	
[C(2)–C(3)–Fe(2)][f]			117.44(31)
C(1)–C(2)–O(1)	121.63(31)	122.49(70)	
[C(2)–C(3)–O(1)][f]			120.17(46)
Fe(2)–C(2)[C(3)][f]–O(1)	120.85(30)	119.77(61)	122.33(42)

[a] Cp1: centroid of C(11)–C(15) for (**1**) and (**3**), C(10)–C(14) for (**2**). [b] Cp2: centroid of C(21)–C(25) for (**1**) and (**3**), C(20)–C(24) for (**2**). [c] For complex (**2**). [d] CP1: centroid of C(11)–C(15) for (**1**) and (**3**), C(10)–C(14) for (**2**). [e] CP2: centroid of C(21)–C(24) for (**1**) and (**3**) and C(20)–C(24) for (**2**) [f] For complex (**3**).

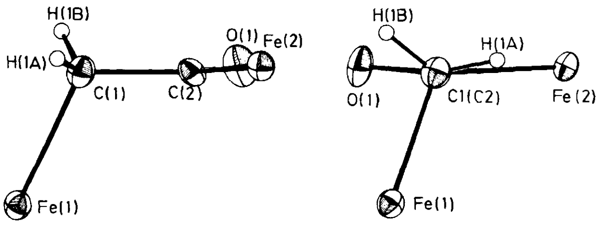

Figure 4. Geometry of the bridging ketene ligand of complex (**1**)

Table 7. Structural parameters for various β-oxoalkyl complexes*

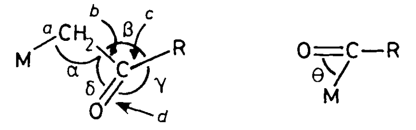

Complex	*a*	*b*	*c*	*d*	α	β	γ	δ	θ
(**1**)	2.073	1.481	2.008	1.219	113.99	117.08	120.85	121.63	76
(**2**)	2.068	1.474	2.002	1.208	115.08	117.63	119.77	122.49	68
(**3**)	2.071	1.534	1.992	1.203	114.61	117.44	122.33	120.17	79
[$(OC)_2$(η^5-C_5H_5)Fe($CH_2COC_5H_4$)Fe(η^5-C_5H_5)]	2.101	1.445	1.471	1.227	110.2	120.4	118.1	121.4	90
	2.094	1.473	1.499	1.233	109.3	120.1	117.8	122.1	89
[Fe(η^5-C_5H_5)$(CO)_2$(CH_2CO_2H)]	2.06	1.42	1.32	1.32	108.2	124.1	123.2	112.7	89
[Mo(η^5-C_5H_5)$(CO)_3$(CH_2CO_2H)]	2.36	1.48	1.24	1.31	106.2	124.0	121.4	113.0	75, 93
[Co$(CO)_3$(PPh_3)($CH_2CO_2CH_2Ph$)]	2.109	1.40	1.42	1.19	111.6	109.1	119.5	130.7	84
[Mn$(CO)_4$(PPh_3)(CH_2COMe)]	2.210	1.453	1.523	1.216	109.1	117.8	118.7	123.5	88
[Ru_2(η^5-C_5H_5)$_2$(μ-CH_2CO)$(CO)_3$]	2.194	1.450	2.105	1.213	89.0	107.6			55
[Os_3(μ-CH_2CO)$(CO)_{12}$]	2.22	1.47	2.16	1.26	112.2	121.4	120.6	117.9	97

* Lengths in Å, angles in °. For complex (**3**): CH_2–CH_2CO 1.519 Å, CH_2–CH_2–CO 117.44°.

overlap between the electron-diffusing Fe–CH_2 bond and the electron-deficient *p* orbital of the acyl carbon as shown in Figure 4, in other words to delocalize the bonding electron by the contribution of (**C**), although such a conformation is frequently observed for organic carbonyl compounds and the θ value of (**3**) (78.8°) lacking a suitable resonance form for back donation from the $Fe(\eta^5-C_5H_5)(CO)_2$ group on the alkyl side is similar to that in (**1**) and (**2**). Such observations have been reported for β-oxoalkyl metal complexes (metal C-enolates) as shown in Table 7.

The geometry of the μ-ketene ligands in complexes (**1**) and (**2**) is essentially the same as those of hitherto reported μ-η^2-(C,C)-ketene complexes, $[Ru_2(\eta^5-C_5H_5)_2(\mu-CH_2CO)(CO)_3]$[6] and $[Os_3(\mu-CH_2CO)(CO)_{12}]$[5] except for unusual dihedral angles owing to linkage of the metal atoms bonded to the μ-ketene ligands by metal–metal bonds. Shortening of the CH_2–CO bond and elongation of the C=O bond indicates the presence of a contribution from the π-complex resonance form (**C**), which is also confirmed by i.r. studies.[3]

Based on the result of an extended-Hückel molecular orbital calculation by Hoffmann and co-workers,[19] in the $M(\eta^5-C_5H_5)(CO)_2$–X type complexes the *a''* orbital plays a dominant role in determining the orientation of π-acidic ligands. Thus, a carbene ligand and an olefinic ligand tend to appear in the 'upright' and 'bisecting' conformations, respectively. The contribution of the oxycarbene resonance form (**B**) observed for complexes (**1**)—(**3**) suggests that the acyl parts adopt the 'upright' conformation, which has actually been observed for complexes containing a strong π acceptor such as $:CR_2$[20] or an electron-donating ancillary ligand such as $Ph_2PCH_2CH_2PPh_2$.[21] The torsion angles between CP2–Fe(2) [CP2: centroid of C(21)–C(25) for (**1**) and C(20)–C(24) for (**2**)] and C(2)-[C(3)]–O(1) are 90.26 (**1**), 81.92 (**2**), and 94.80° (**3**), which correspond to the 'bisecting' conformation, contrary to expectation. On the other hand, the π-resonance form (**C**) should lead to the 'bisecting' conformation around Fe(1). However, the dihedral angles between the CP1–Fe(1) [CP1: centroid of C(11)–C(15) for (**1**) and C(10)–C(14) for (**2**)] and C(1)–C(2) planes are 166.64 (**1**) and 169.51° (**2**), respectively, and CP1 and C(2) are located in the antiperiplanar conformations. Thus in the solid state the geometry around the metal centres is determined by the need to minimize steric repulsions, and does not reflect orbital interactions.

Acknowledgements

This work was financially supported by the Asahi Glass Foundation for Industrial Technology and the Ministry of Education, Science, and Culture of Japan. Special thanks are due to Professor H. Suzuki for helpful discussions on the *X*-ray structure analyses.

References

1 G. L. Geoffroy and S. L. Bassner, *Adv. Organomet. Chem.*, 1988, **28**, 1.

2 G. Blyholder and P. H. Emmett, *J. Phys. Chem.*, 1960, **64**, 470; M. Ichikawa, K. Sekizawa, K. Shikakura, and M. Kawai, *J. Mol. Catal.*, 1981, **11**, 137; A. Takeuchi and J. R. Katzer, *J. Phys. Chem.*, 1982, **86**, 2438; P. H. McBreen, W. Erley, and H. Ibach, *Surf. Sci.*, 1984, **148**, 1292.

3 M. Akita, A. Kondoh, and Y. Moro-oka, *J. Chem. Soc., Chem. Commun.*, 1986, 1296; M. Akita, A. Kondoh, T. Kawahara, T. Takagi, and Y. Moro-oka, *Organometallics*, 1988, **7**, 366.

4 J. K. P. Ariyaratne, A. M. Bierrum, M. L. H. Green, M. Ishaq, C. K. Prout, and M. G. Swanwick, *J. Chem. Soc. A*, 1969, 1309.

5 E. D. Morrison, G. R. Steinmetz, G. L. Geoffroy, W. C. Fultz, and A. L. Rheingold, *J. Am. Chem. Soc.*, 1984, **106**, 4783.

6 N. M. Doherty, M. J. Fildes, N. J. Forrow, S. A. R. Knox, K. A. Macpherson, and A. G. Orpen, *J. Chem. Soc., Chem. Commun.*, 1986, 1355.

7 M. Akita, N. Kakinuma, and Y. Moro-oka, *J. Organomet. Chem.*, 1988, **348**, 91.

8 'International Tables for *X*-Ray Crystallography,' Kynoch Press, Birmingham, 1974, vol. 4.

9 V. B. Rybakov, L. A. Aslanov, V. M. Ionov, and S. A. Eremin, *J. Struct. Chem. (Engl. Transl.)*, 1983, **24**, 230.

10 M. J. Bennett, jun., F. A. Cotton, A. Davison, J. W. Fackler, S. J. Lippard, and S. M. Morehouse, *J. Am. Chem. Soc.*, 1966, **88**, 4371.

11 L. Pope, P. Sommerville, and M. Laing, *J. Organomet. Chem.*, 1976, **112**, 309.

12 M. R. Churchill and J. Wormald, *Inorg. Chem.*, 1969, **8**, 1936.

13 H. Blau, W. Malish, S. Voran, K. Blank, and C. Kruger, *J. Organomet. Chem.*, 1980, **202**, C33.

14 M. E. Wright, G. O. Nelson, and R. S. Glass, *Organometallics*, 1985, **4**, 245.

15 J. March, 'Advanced Organic Chemistry: Reactions, Mechanisms, and Structure,' McGraw-Hill International, Tokyo, 1977, p. 24.

16 F. A. Cotton, B. A. Frenz, and A. Shaver, *Inorg. Chim. Acta*, 1973, **7**, 161.

17 T. G. Attig, R. G. Teller, S-M. Yu, R. Bau, and A. Wojcicki, *J. Am. Chem. Soc.*, 1979, **101**, 619.

18 V. A. Semion and Y. T. Struchkov, *J. Struct. Chem. (Engl. Transl.)*, 1969, **10**, 563.

19 B. E. R. Schilling, R. Hoffmann, and D. L. Lichtenberger, *J. Am. Chem. Soc.*, 1979, **101**, 585.

20 A. M. Crespi and D. F. Shriver, *Organometallics*, 1985, **4**, 1830.

21 H. Felkin, B. Meunier, C. Pascard, and T. Prange, *J. Organomet. Chem.*, 1977, **135**, 361.

Received 27*th July* 1988; *Paper* 8/03067G